The Development of Zeolite-Entrapped Organized Molecular Assemblies

James R. Kincaid[a]

Abstract: A brief summary is presented of the development of organized molecular assemblies entrapped within the supercages of Y-zeolite. Emphasis is placed on work originating in the author's laboratory, although a discussion of some of the important contributions made by other workers, which inspired and facilitated this work, are included. Following pioneering studies by Lunsford and co-workers, which demonstrated the feasibility of encapsulating the common photosensitizer $[Ru(bpy)_3]^{2+}$ within the Y-zeolite supercage, Dutta and co-workers documented efficient photoinduced electron transfer to viologen acceptors occupying neighboring supercages. We have extended the range of available materials by developing synthetically versatile methods to permit the incorporation of heteroleptic complexes, including constituent ligands which contain peripheral nitrogen donor groups; for example , 2,2′-bipyrazine. In an impressive study employing zeolite-excluded acceptors, Dutta and co-workers showed that the reducing equivalents available from photoinduced electron transfer from the zeolite entrapped sensitizer to intra-zeolite acceptors could be transferred to the extra-zeolite acceptors in aqueous suspensions, although the net charge-separation efficiency was low, presumably because of a persistent relatively efficient back-electron transfer process involving the primary photoproduct; that is, the entrapped sensitizer–acceptor dyad. Exploiting the susceptibility of certain heteroleptic complexes to add reactive ruthenium reagents, methods were developed to construct spatially organized donor–sensitizer–acceptor triads within the supercage framework of Y-zeolite. Such assemblies exhibit dramatically improved net charge-separation efficiencies, presumably as a consequence of inhibiting the wasteful back-electron transfer reaction between the initial sensitizer–acceptor couple.

Keywords: electron transfer · photochemistry · zeolites

[a] Prof. J. R. Kincaid
Chemistry Department
Marquette University
Milwaukee, WI 53233 (USA)
Fax: (+1) 414-288-7066

Introduction

There is intense interest in designing molecular systems that mimic photosynthesis since these may be used to capture sunlight reaching the earth's surface and convert the energy to useful chemical fuels.[1–5] Nature accomplishes its complex photocatalytic cycle by precise arrangement of individual components so as to maximize the efficiency of each step. A corresponding synthetic system capable of producing H_2 by photochemical reduction of water, coupled to a water oxidation cycle is shown schematically in Scheme 1. Here a

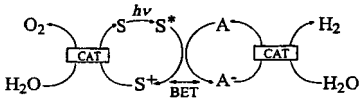

$$S \xrightarrow{h\nu} S^*$$
$$S^* + A \longrightarrow S^+ + A^-$$

Scheme 1. Schematic for a synthetic water-splitting system.

photosensitizer, excited by absorption of visible light, forms a sufficiently long-lived excited state to undergo an electron transfer reaction with a suitable primary acceptor molecule (A) to generate S^+ and A^-. As long as the redox potentials of S^+ and A^- are adequate to oxidize and reduce H_2O, the system is thermodynamically competent for the splitting of H_2O into H_2 and O_2.

Of the several classes of molecules that have been shown to possess the necessary properties to serve as effective photosensitizers for such schemes, the most promising are those based on polypyridine complexes of divalent ruthenium (i.e., $[Ru(bpy)_3]^{2+}$ (bpy = 2,2′-bipyridine) and related complexes) and various metal complexes (MP) of tetrapyrrole macrocycles such as porphyrins and phthalocyanines.[6] However, even though suitable photosensitizers are available, there are several fundamental problems which need to be overcome in order to make Scheme 1practical.

Once the initial photoinduced electron transfer event is completed to form S^+ and A^-, there is a large driving force for the back electron transfer (BET) reaction and steps must be taken to minimize or eliminate this wasteful process. This is most effectively accomplished by incorporation of a donor molecule which is of appropriate redox potential and suitably

  0947-6539/00/0622-4055 $ 17.50+.50/0

positioned to rapidly reduce the S^+ to S before the BET step can occur. The other major difficulty is the fact that the photon-induced electron transfer processes are single-electron transfer events, while the water splitting reactions are multielectron transfer reactions. Thus, the oxidation and reduction equivalents centered on the initial photoredox products (S^+ and A^-) need to be separated from one another and coupled with catalysts suitable for production of H_2 and O_2.

Clearly, a sophisticated level of molecular organization, mimicking the natural photosynthetic apparatus, will be required to accomplish these difficult tasks. Of course, given the undeniable importance of the ultimate goal, there has been intense interest and extensive work in designing effective organizational strategies. These include the synthesis of covalently linked redox assemblies[7] and the use of various supports.[2–5, 8] One of the most attractive approaches involves the use of highly ordered host materials, such as zeolites, and herein some of the promising results which have been obtained with these materials are summarized.

Synthesis and Characterization of Zeolite-Entrapped Photosensitizers

Zeolite structures

Zeolites are aluminosilicates having the general chemical formula $M_{2/n}O \cdot Al_2O_3 \cdot x\,SiO_2 \cdot y\,H_2O$.[910] The three-dimensional structure is made up of corner-sharing SiO_4 and AlO_4 tetrahedra, with the cations M^{n+} occupying extra framework positions to balance the charge of the AlO_4 units. Interconnecting cages and channels make up the internal structure of a zeolite particle and frameworks with many different topologies (over 100) have been synthesized.[9, 10] However, given the size of the most promising sensitizers for photocatalytic applications, much interest has been focused on Y-zeolite (a so-called faujasitic type zeolite), the structure of a single "supercage" of which is shown in Figure 1.

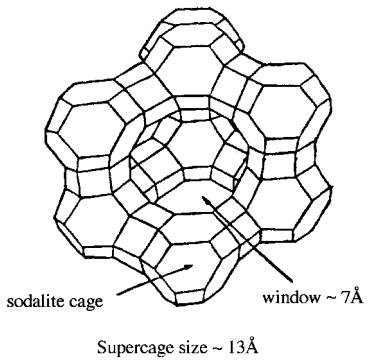

Figure 1. The structure of a zeolite-Y supercage.

The framework consists of sodalite cages which are connected in a tetrahedral arrangement through "double 6-rings" to produce a three-dimensional network. This arrangement gives rise to supercages of ≈ 13 Å internal diameter, connected to each other through 12-membered ring openings having "windows" of 7 – 8 Å in diameter. Each supercage is connected to four other (tetrahedrally arranged) supercages to form a continuous three-dimensional framework of interconnecting supercages. In order to clarify later descriptions, it is noted that the four supercages surrounding the central cage do not share a common window with any of the other four (i.e., these four supercages are not adjacent to one another).

Synthesis and properties of zeolite-entrapped $[Ru(bpy)_3]^{2+}$ and related complexes

Synthesis: Lunsford and co-workers[11] were the first to show that $[Ru(bpy)_3]^{2+}$ could be synthesized and entrapped within the supercages of Y-zeolite by a "ship-in-the-bottle" approach and the method was later extended and refined by Dutta and his group[8] and by Calziferri and co-workers,[12] as illustrated in Scheme 2.

Zeolite (Z) + $Ru(NH_3)_6^{3+}$

aqueous suspension ↓ ion-exchange

↓ filter, dry

Z-$[Ru(NH_3)_6]^{3+}$

excess bpy ↓ 200°C (sealed tube)

crude Z-$[Ru(bpy)_3]^{2+}$ (plus bpy degradation products)

↓ NaCl wash

↓ soxhlet extraction (95% ethanol)

pure Z-$[Ru(bpy)_3]^{2+}$

Scheme 2.

The initial zeolite sample (Z) is loaded with $[Ru(NH_3)_6]^{3+}$ by simple ion-exchange from a solution of $[Ru(NH_3)_6]^{3+}$, filtered, and dried on a vacuum line. During the high-temperature treatment with excess bipyridine, in a sealed tube, the color of the solid changes from white to bluish-red to yellow. Surface-adsorbed $[Ru(bpy)_3]^{2+}$ is easily removed by washing with 10 % NaCl solution, while excess ligand, and any other organic by-products, can be removed by exhaustive soxhlet extraction with 95 % ethanol or other solvents. The color changes occurring during the heating step were not reported in the original work.[8, 11] However, in our early attempts to prepare this material the bluish-red color was noted and was interpreted to be a consequence of the intermediate formation of the bis-bpy precursor, $[Ru(bpy)_2(H_2O)_2]^{2+}$. This conclusion was verified and led to the development of a reliable method for the preparation of pure samples of zeolite-entrapped $[RuL_2(H_2O)_2]^{2+}$ (where L is a polypyridine ligand; see Equation (1)].[13, 14] This crude material can be purified in the same manner described for Z-$[RuL_3]^{2+}$ complexes without generating significant amounts of the tris-ligated species.

$$Z\text{-}[Ru(NH_3)_6]^{3+} + L \xrightarrow[12\,h]{90\,^\circ C} \textit{crude}\ Z\text{-}[RuL_2(H_2O)_2]^{2+} \quad (1)$$

0947-6539/00/0622-4056 $ 17.50+.50/0 *Chem. Eur. J.* **2000**, *6*, No. 22

The availability of pure samples of zeolite-entrapped, bis-polypyridine complexes provided an entry for the synthesis of tris-ligated heteroleptic complexes, according to the procedure in Equation (2), [13, 14] where L and L′ are two different polypyridine ligands.

$$Z\text{-}[RuL_2(H_2O)_2]^{2+} + L' \text{ (large excess)} \xrightarrow[18\,h]{180\,^\circ C} \textit{crude } Z\text{-}[RuL_2L']^{2+} \qquad (2)$$

Purification by conventional methods (NaCl wash and soxhlet extraction) yields pure samples of Z-$[RuL_2L']^{2+}$. The integrity of the materials is confirmed by comparison of chromatographic and spectroscopic data for solutions of the authentic complexes with those of the liberated complexes; that is, aqueous acid dissolves the zeolite framework.

The ability to generate zeolite-entrapped, heteroleptic tris-ligated complexes (i.e., Z-$[RuL_2L']^{2+}$) provided access to a wide range of materials which were suitable for a systematic evaluation of the effects of the zeolite matrix on inherent photophysical properties, as is summarized in the next section. Of greater significance is that fact that some of these materials are suitable precursors for synthetic elaboration of such systems, thus promising to offer a practical vehicle to the more sophisticated level of organization which is required to devise efficient photoredox assemblies (vide infra).

Effects on photophysical properties

To the extent that zeolite-based photoredox assemblies are potentially useful materials, it is quite important to gain an understanding of the interactions of various entrapped species with each other and with the host framework. The early studies of the reference material Z-$[Ru(bpy)_3]^{2+}$ indicated that the inherent photophysical properties of $[Ru(bpy)_3]^{2+}$ are not substantially altered by entrapment within the zeolite supercages.[8, 11] Thus, the diffuse reflectance and emission spectra were only slightly different from those of the free complex in solution. Lifetime measurements (at room temperature) also yielded a value ($\approx$610 ns) comparable to that exhibited by aqueous solutions of the free complex (i.e., $\approx$600 ns).

On the other hand, in the extended series of materials containing tris-ligated complexes of other polypyridine ligands (e.g. Z-$[Ru(bpz)_3]^{2+}$) and those containing bis-heteroleptic, tris-ligated complexes (e.g. Z-$[RuL_2L']^{2+}$), rather dramatic alterations in photophysical properties were observed for the zeolite-entrapped species, relative to those of the free complexes. [13, 14] Thus, both red and blue shifts in the λ_{max} and λ_{em} peaks were noted for various complexes and lifetimes were observed to either increase or decrease, dramatically so in certain cases. Based on thorough (temperature-dependent) lifetime and spectroscopic measurements of a rather extensive series of complexes,[13–18] a self-consistent and reliable framework has been devised for interpretation of these zeolite- induced alterations, the major effects being interactions of the polar zeolite framework with peripheral heteroatoms of ligands such as 2,2′-bipyrazine (bpz), and steric restrictions to elongation of the Ru–N bonds in the so-called ligand-field (LF), or ^{3}dd, state. In solution this state is thermally accessible from the metal-to-ligand charge transfer (^{3}MLCT) state, whereas within the zeolite supercage the energy of the LF state often is sufficiently increased to render it inaccessible at room temperature.[13–17] In fact, this interpretational framework reliably predicts the observed (very dramatic) increase in the ^{3}MLCT state lifetime (from $>$10 ns in solution to over 300 ns in the zeolite-entrapped species) for the complex, $[Ru(bpy)_2(daf)]^{2+}$ (where daf is diazafluorene).[15] The daf ligand possesses such a weak ligand field strength that the LF state is only $\approx$2300 cm^{-1} above the ^{3}MLCT state in free solution. Careful measurements and analysis of lifetime data over a large temperature range yielded a (^{3}MLCT-LF) energy gap of $\approx$4000 cm^{-1} in the case of the zeolite entrapped complex as illustrated in Figure 2;

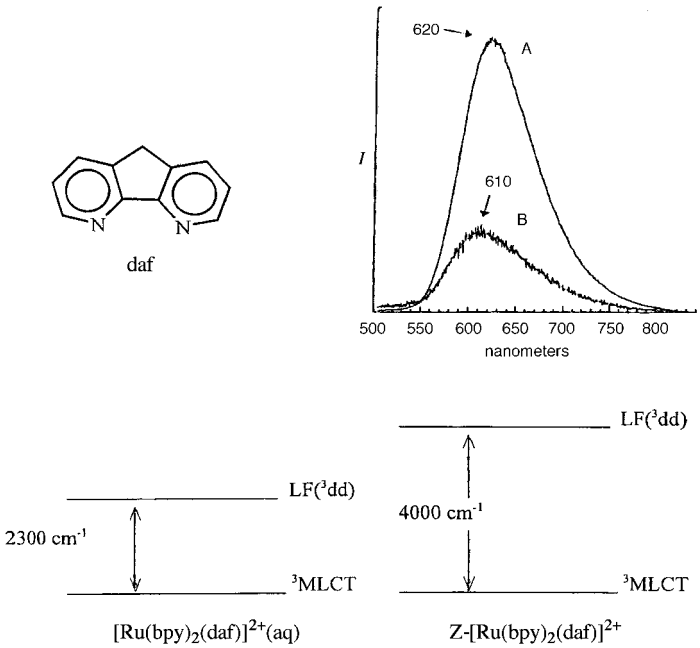

Figure 2. Photophysical properties of Z-$[Ru(bpy)_2(daf)]^{2+}$. A = emission spectrum of zeolite-entrapped complex, B = emission spectrum of complex in solution.

that is, elimination of the LF state decay pathway leads to the dramatic increase in the observed lifetime and emission intensity.

A similar, but even more dramatic increase in the ^{3}MLCT state lifetime of the bis-terpyridine(tpy) complex $Ru(tpy)_2^{2+}$ upon incorporation into Y-zeolite has verified this effect.[17] This complex has an extremely short ^{3}MLCT state lifetime of 250 ps in aqueous solution at room temperature, the rapid decay being most reasonably attributed to a very low-lying LF state.[19] The corresponding zeolite-entrapped complex Z-$[Ru(tpy)_2]^{2+}$, emits very strongly at room temperature and exhibits a ^{3}MLCT state lifetime of over 100 ns, an increase by a factor of almost 1000.

Zeolite-Based Photoredox Assemblies

The advantage of compartmentalization

One of the first documented uses of zeolites to construct a multicomponent photocatalytic assembly was the elegant

work reported by Mallouk and co-workers,[20] a schematic of which is shown below. The particular zeolite used in this work was zeolite L, which has a one-dimensional tunnellike structure. Methods were developed to form small platinum clusters *inside* the zeolite channel and it was subsequently loaded with a large amount of methyl viologen acceptor (MV^{2+}) (see Scheme 3). The zinc porphyrin photosensitizer used, $[ZnTMPyP]^{4+}$ (TMPyP = tetramethylpyridinium porphyrin), is too large to penetrate into the 7 Å zeolite-L channels and, instead, is ion-exchanged onto the zeolite surface.

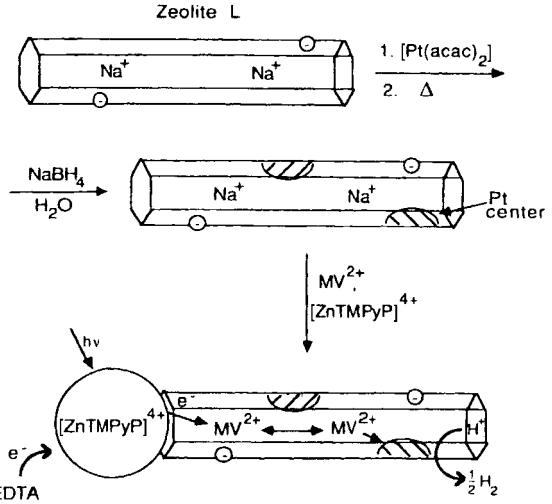

Scheme 3. Synthesis of an early zeolite-based multicomponent photocatalytic assembly.[20]

In the presence of a sacrificial electron donor, EDTA, this system was shown to be capable of photocatalytic evolution of H_2. Thus, at pH 4, the solution-phase EDTA is negatively charged and intimately associated with the adsorbed sensitizer $[ZnTMPyP]^{4+}$. Upon photolysis, the singlet state of the porphyrin is quenched by the neighboring intrazeolitic viologen molecules, and the sacrificial electron donor, EDTA, is oxidized by the zinc porphyrin cation radical. This reductive quenching of the oxidized sensitizer effectively prevents ($MV^{+\bullet}$ to $[ZnTMPyP]^{5+}$) back electron transfer. The resulting long-lived $MV^{+\bullet}$ transfers its reducing equivalents along the chain of MV^{2+} molecules which fill the zeolite L channel. In the presence of the Pt catalyst, H_2 is evolved.

Binary photoredox systems involving ruthenium polypyridine sensitizers

At about this same time, Dutta and co-workers[8, 21] were investigating photoredox processes for $[Ru(bpy)_3]^{2+}$-loaded zeolite-Y particles which also contained saturating amounts of the acceptor MV^{2+}. That is, in these particles, all of the cages surrounding an isolated, entrapped $[Ru(bpy)_3]^{2+}$ photosensitizer are filled with MV^{2+} (Figure 3). In fact, at these high loadings of MV^{2+}, almost every supercage contains two MV^{2+} molecules.

When this solid was photolyzed in an anaerobic environment, a blue color was observed, a color indicative of $MV^{+\bullet}$. The presence of the viologen radical was confirmed by

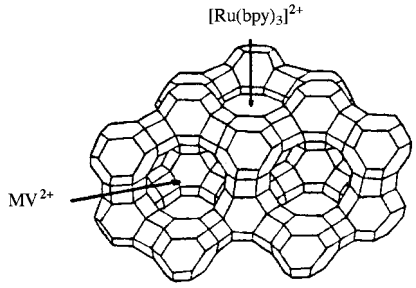

Figure 3. A zeolite-entrapped sensitizer – acceptor dyad.[21]

resonance Raman (RR) spectroscopy, the RR spectrum exhibiting bands characteristic of the reduced viologen. In the absence of oxygen this species was stable for several hours. In a later study,[22] using lower concentrations of $[Ru(bpy)_3]^{2+}$ in the particle, the nature of the quenching process (i.e., electron transfer quenching of the ^{3}MLCT state, $[\{Ru(bpy)_3\}^{2+}]^*$, by MV^{2+}) was studied by varying the concentration of MV^{2+} in the particle. In the photolyzed samples, $MV^{+\bullet}$ was observed by diffuse reflectance spectroscopy to increase with photolysis time. The results were interpreted to indicate that the back electron transfer from $MV^{+\bullet}$ to $[Ru(bpy)_3]^{3+}$ was inhibited by a static quenching mechanism, whereby the primary photogenerated $MV^{+\bullet}$ transfers its electron to more remote MV^{2+} acceptors. In two impressive related studies Mallouk and co-workers[23, 24] used time-resolved diffuse reflectance (TRDR) spectroscopy to investigate the kinectics of photoelectron transfer processes in zeolites which had been loaded with methyl viologen in the interior and $[Ru(bpy)_3]^{2+}$ adsorbed to the surface. These workers found that the rate of back electron transfer at the zeolite surface is dramatically lowered relative to the rate observed in solution.

Ternary photoredox systems

While the studies described above clearly demonstrate the capability to attain relatively long-term charge separation, the photogenerated reducing equivalents remain trapped inside a given zeolite particle and charge recombination eventually occurs. In order to devise practical systems it is necessary to access this chemical potential by facilitating charge transfer out of the particle into solution. One method to accomplish this, which was performed by Dutta and Borja,[25] is outlined in Figure 4. In this system, a neutral viologen (PVS) was placed into the solution phase of a suspension which included zeolite particles loaded with $[Ru(bpy)_3]^{2+}$ and a viologen (DQ^{2+}) of relatively high reduction potential (−0.65 V) compared to PVS (−0.41 V). Upon electron transfer quenching of the ^{3}MLCT state of $[Ru(bpy)_3]^{2+}$, the $DQ^{+\bullet}$ radical generated is capable of reducing the zwitterionic neutral viologen, PVS, whose reduction potential (−0.41 V) is lower than that of DQ^{2+}. Photolysis with visible light (200 mW of 400 – 600 nm light) generates the blue anion radical of PVS (i.e., $PVS^{-\bullet}$) in the solution phase. In addition to providing the first example of a photochemical assembly that leads to permanent charge separation in the absence of a sacrificial electron donor, this system also provides a more convenient means to measure

0947-6539/00/0622-4058 $ 17.50+.50/0 *Chem. Eur. J.* **2000**, *6*, No. 22

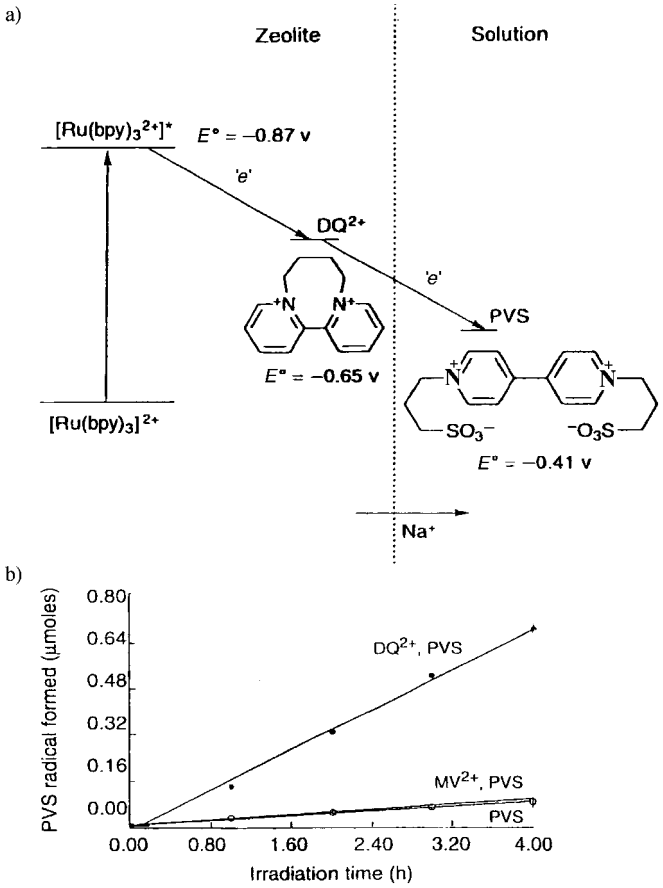

Figure 4. A zeolite-entrapped sensitizer–acceptor dyad with excluded viologen. a) Method for facilitating charge transfer out of a zeolite into a solution. See text for details.[25] b) Comparison of growth of PVS^- in suspensions of zeolitic materials with 0.01 M PVS in solution. Curves shown for photolysis of Z-$[Ru(bpy)_3]^{2+}$, Z-$[Ru(bpy)_3]^{2+}$ loaded with MV^{2+} and Z-$[Ru(bpy)_3]^{2+}$ loaded with DQ^{2+}.

photochemical quantum yields, compared to photolysis of solid samples. This is so because the net production of viologen radical can be more accurately determined (by absorption spectrophotometry of the solution containing the excluded viologen product) and a relatively reliable approximation of the number of absorbed photons can be obtained by comparing the transmitted light with that observed for an identical experimental arrangement using suspensions of plain zeolite (i.e., no intrazeolite species present). In the particular case described (i.e., the $[Ru(bpy)_3]^{2+}/DQ^{2+}/PVS$ system), the photochemical quantum yield for $PVS^{-\bullet}$ production was estimated to be $\approx 5 \times 10^{-4}$.These disappointingly low photochemical quantum yields reflect the combined inefficiencies of several key steps in the overall cycle, the natural tendency for the initial charged-separated pair (e.g., $[Ru(bpy)_3]^{3+} \cdot DQ^{+\bullet}$) to undergo the wasteful BET reaction being one of the important obstacles.

More highly organized systems—dramatically enhanced photoredox efficiencies

Synthesis of zeolite-based organized molecular assemblies: One strategy to overcome the fundamental limitation involving the BET reaction is to include a donor molecule in the photochemical cycle, as was pointed out earlier in discussing Scheme 1. In order for this approach to be effective the donor must not only have an appropriate redox potential (i.e., D^+ must be favored over $[Ru(bpy)_3]^{3+}$), but the system must also be spatially organized so as to facilitate rapid electron transfer to reduce the oxidized sensitizer. The major deficiency which had plagued zeolite-based photochemical systems until recently was the inability to attain this degree of spatial organization, all earlier systems having been prepared by ion-exchange or simple adsorption; methods which give rise to a randomized arrangement of components. What was needed was a synthetic scheme which would allow controlled positioning of the individual components within the existing zeolite framework.

Recognizing the fact that these zeolite-entrapped, heteroleptic polypyridine complexes offered a possible route to the construction of such materials, attention in our laboratory over the past few years has focused on developing the necessary synthetic methods for organizational elaboration of zeolite-entrapped catalytic assemblies;[26–29] one example is illustrated in Figure 5.

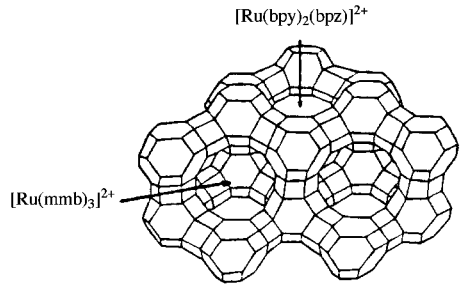

Figure 5. A zeolite-entrapped "adjacent cage" dyad.[26]

An effective synthetic scheme, which exploits the susceptibility of coordinated 2,2′-bipyrazine (bpz) and similar ligands to attachment of secondary metal complexes,[30] is outlined in Scheme 4. Briefly, a zeolite sample loaded with, for example,

Z-$[Ru(bpy)_2(bpz)]^{2+}$ + $[(H_2O)Ru(NH_3)_5](PF_6)_2$ (large excess)

↓ acetone, anaerobic

crude Z-$[Ru(bpy)_2(bpz\text{-}Ru(NH_3)_5)^{4+}]$

↓ NaCl wash, anaerobic

pure Z-$[Ru(bpy)_2(bpz\text{-}Ru(NH_3)_5)^{4+}]$

↓ mmb (large excess), 180°C, sealed tube

crude Z-$[Ru(bpy)_2(bpz)]^{2+}$ / $[Ru(mmb)_3]^{2+}$

↓ soxhlet extraction (95% ethanol)

pure Z-$[Ru(bpy)_2(bpz)]^{2+}$ / $[Ru(mmb)_3]^{2+}$

Scheme 4.

$[Ru(bpy)_2(bpz)]^{2+}$ is treated with an acetone solution of $[(H_2O)Ru(NH_3)_5](PF_6)_2$, whereupon a $Ru(NH_3)_5^{2+}$ fragment is attached to one of the peripheral nitrogens of the

coordinated bipyrazine to form Z-[Ru(bpy)$_2$(bpz-Ru(NH$_3$)$_5$)$^{4+}$]. This material, when treated with excess 5′-monomethyl-2,2′-bipyridine (mmb), yields a zeolite sample which contains dyad units, wherein two complexes are entrapped in neighboring supercages; that is, (Z-[Ru(bpy)$_2$(bpz)]$^{2+}$/[Ru(mmb)$_3$]$^{2+}$). Thorough spectroscopic and photophysical studies of this and similar systems document the integrity of the entrapped species and provide convincing evidence for a strong electronic interaction between the adjacent cage complexes.[26–29, 31]

The effectiveness of the synthetic procedure outlined above relies on the stability of an intermediate species; for example, zeolite-entrapped [Ru(bpy)$_2$bpz-Ru(NH$_3$)$_5$]$^{4+}$. Treatment of this material with an excess of another polypyridine ligand (e.g., mmb) results in adjacent cage assemblies only to the extent that the detached [Ru(NH$_3$)$_5$]$^{2+}$ fragment does not drift to another cage before being captured by the excess mmb ligands to form the tris-mmb complex in the cage adjacent to the original [Ru(bpy)$_2$(bpz)]$^{2+}$ complex. While the results summarized in the above-cited works provided strong indirect evidence for the effectiveness of the synthetic scheme developed, in order to provide further, more direct, support for the efficiency with which the secondary complex is indeed trapped within the adjacent cage, studies were carried out for the zeolite-entrapped [Ru(bpy)$_2$(pypz)]$^{2+}$ complex (pypz is pyridylpyrazine), wherein the primary complex contains only one peripheral heteroatom. To the extent that rotation is restricted for an entrapped tris-ligated complex, the application of a two-cycle reaction sequence should yield no reaction with the second treatment of [(H$_2$O)Ru(NH$_3$)$_5$]$^{2+}$; that is, if the adjacent cage entrapment is 100 % efficient, further access to the peripheral nitrogen is expected to be blocked by the secondary complex. The synthesis and detailed characterization of the zeolite-entrapped primary complex, Z-[Ru(bpy)$_2$(pypz)]$^{2+}$, have been published[16] and, recently, we have obtained pure samples of the zeolite-entrapped adjacent cage pair, Z-[Ru(bpy)$_2$(pypz)]$^{2+}$/[Ru(bpy)$_3$]$^{2+}$. Most significantly, treatment of this latter material with an excess of [(H$_2$O)Ru(NH$_3$)$_5$]$^{2+}$ yields a product whose absorption spectrum is virtually identical to that of the adjacent cage material; that is, only traces of an absorption characteristic of the [pypz-Ru(NH$_3$)$_5$]$^{2+}$ fragment could be detected, indicating that the single peripheral nitrogen atom of the primary complex is now effectively shielded from further reaction. These results[29] therefore quite convincingly document the high efficiency of the adjacent cage dyad formation, confirming the fact that upon detachment from the primary complex, the [Ru(NH$_3$)$_5$]$^{2+}$ fragment does not migrate to more remote cages, but instead, reacts with polypyridine ligands present in the cage adjacent to the primary complex [Ru(bpy)$_2$(pypz)]$^{2+}$.

Enhanced efficiency: As will now be seen, the efficiency of photoinduced charge separation in these zeolite-based systems is indeed greatly improved by organization of the intrazeolitic components. Referring to Figure 6, the essential strategy being employed to increase the charge-separation efficiency is as follows. Similar to the original system developed by Dutta and co-workers[8, 25] (see Figure 4) the photosensitizer ([Ru(bpy)$_2$(bpz)]$^{2+}$, in this case, is surrounded

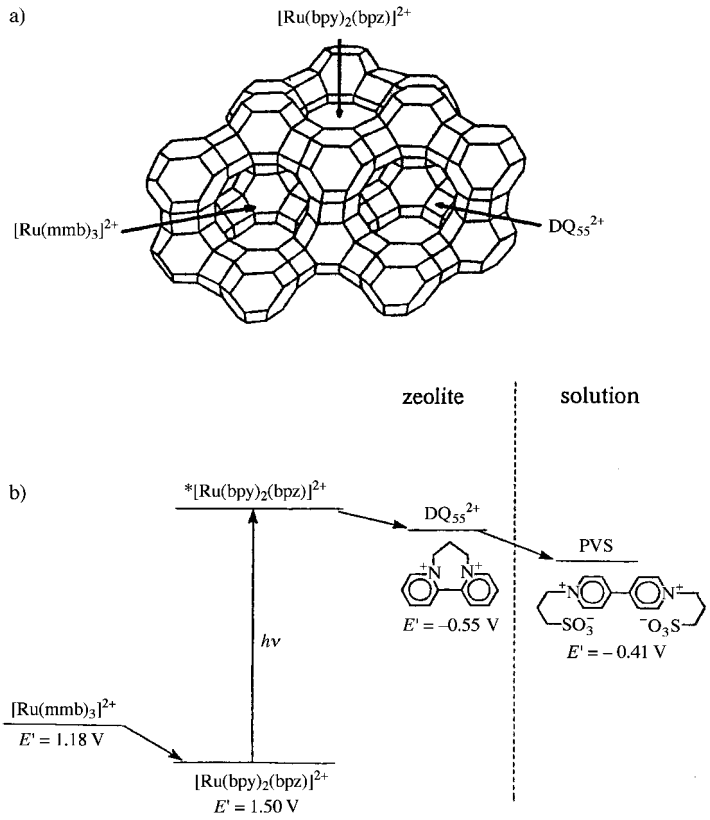

Figure 6. a) A zeolite-entrapped donor–sensitizer–acceptor triad with excluded viologen.[27] b) Outline of the strategy employed to increase the charge-separation efficiency in this system.

by viologen acceptors. In this material, however, the assembly also includes a potential donor component, [Ru(mmb)$_3$]$^{2+}$, properly positioned in the cage adjacent to the sensitizer, and it is noted that the trivalent oxidation state is favored for [Ru(mmb)$_3$]$^{3+}$ over [Ru(bpy)$_2$(bpz)]$^{3+}$. Upon selective excitation (473 nm) of the [Ru(bpy)$_2$(bpz)]$^{2+}$ sensitizer, an initial photoproduct ([Ru(bpy)$_2$(bpz)]$^{3+}\cdot$DQ$_{55}^{+\bullet}$) is formed. Now, to the extent that reductive quenching of the oxidized sensitizer by the [Ru(mmb)$_3$]$^{2+}$ is efficient and rapid, the resulting charge-separated pair ([Ru(mmb)$_3$]$^{3+}\cdot$DQ$_{55}^{+\bullet}$) is separated by an "insulating" (reduced) sensitizer molecule and the undesirable BET reaction should be effectively eliminated.

Figure 7 shows a series of absorption spectra that document the continuous growth of excluded PVS radical in the solution phase upon prolonged irradiation (473 nm) of the system illustrated in Figure 6. The magnitude of this growth, as a function of irradiation time, is plotted in Figure 8 with the curve labeled AC (to signify "adjacent cage" dyad system). Also plotted in Figure 8 is the corresponding curve for an appropriate reference system (MM) consisting of a suspension of a mixture of zeolitic materials in a solution of PVS. The MM reference system contains equal amounts of Z-[Ru(bpy)$_2$(bpz)]$^{2+}$ and Z-[Ru(mmb)$_3$]$^{2+}$, both of which are loaded with saturating levels of DQ$_{55}^{2+}$. It is important to emphasize that the MM reference system contains the same concentrations of both complexes as are present in the adjacent cage dyad system. Thus, the increased efficiency of the AC system, relative to the MM reference system, is directly attributable to the unique *spatial organization* of the

0947-6539/00/0622-4060 $ 17.50+.50/0 *Chem. Eur. J.* **2000**, *6*, No. 22

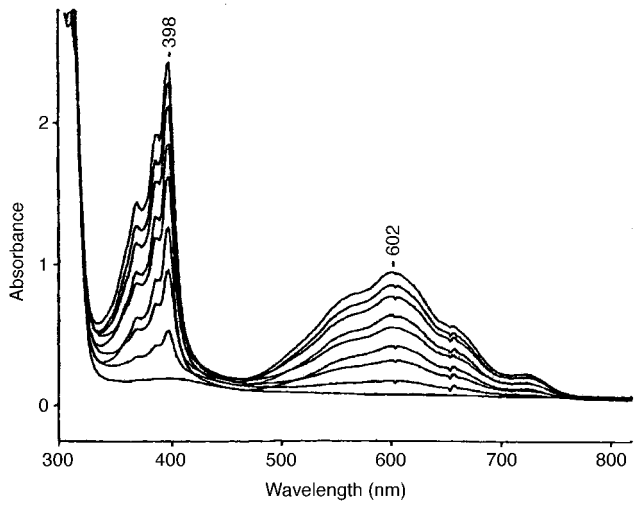

Figure 7. Spectral documentation of solution-phase PVS anion radical production.[27]

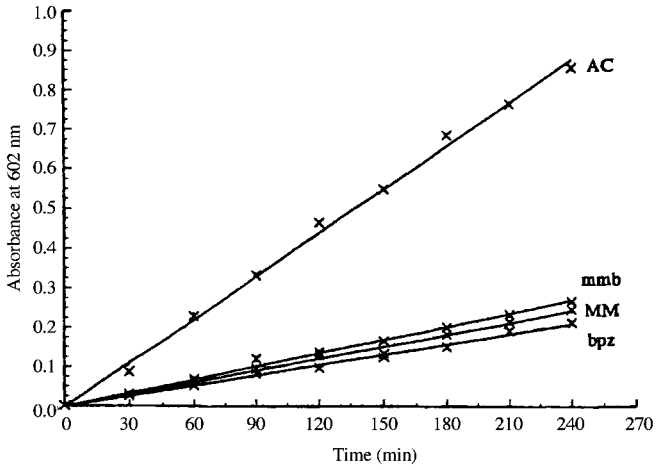

Figure 8. Comparison of PVS radical production for various systems.[27]

two complexes in the sensitizer–donor dyad system. The results of similar studies on isolated systems, Z-[Ru(bpy)$_2$(bpz)]$^{2+}$ and Z-[Ru(mmb)$_3$]$^{2+}$, are also included in Figure 8 and, as expected, are similar to those for the MM reference and that of the system studied earlier by Dutta and Borja.[25]

Conclusion and Future Directions

The above studies clearly demonstrate that the zeolite architecture is well suited for compartmentalization of two or more photoredox components. The early systems were plagued by the essentially random nature of the loading step; that is, various molecular species within the zeolite particle were distributed in a statistical fashion. The development of an effective strategy to create isolated sensitizer/donor dyads within the zeolite framework has led to the desired substantial increases in efficiency for a charge-separation application. However, this synthetic strategy is an important development which provides the higher level spatial organization required to improve the overall photocatalytic efficiency of these materials and it is hoped that this strategy will prove useful for a wide range of applications, including those involving the binding and activation of small molecular reactants, such as dioxygen and the oxides of carbon and nitrogen.

Acknowledgement

The author acknowledges the help and collaboration of Milan Sykora, Krzysztof Maruszewski, and other students and co-workers involved in the work cited herein and expresses his gratitude to Professors P. K. Dutta (Ohio State University) and D. P. Strommen (Idaho State University) for their helpful advice and cooperation. Much of the author's work cited in this article was supported by grant (DE-FG-02–86ER13619) from the United States Department of Energy, Division of Chemical Sciences. The author also thanks the Wehr Foundation for its generous support.

[1] V. N. Parmon, K. I. Zamarev in *Photocatalysis: Fundamentals and Applications* (Eds.: N. Serpone, E. Pelizzetti), Wiley, New York, **1989**, 565–602.
[2] A. J. Bard, M. A. Fox, *Acc. Chem Res.* **1995**, *28*,141.
[3] *Energy Resources Through Photochemistry and Catalysis* (Ed.: M. Gratzel), Academic Press, New York, **1983**.
[4] *Kinetics and Catalysis in Microheterogeneous Systems* (Eds.: M. Gratzel, K. Kalyanasundarum), Marcel Dekker, New York, **1991**.
[5] *Photochemistry in Organized and Constrained Media* (Ed.: V. Ramamurthy), VCH, New York, **1991**.
[6] Kalyanasundarum, *Photochemistry of Polypyridine and Porphyrin Complexes*, Academic Press, London **1992**.
[7] D. Gust, T. A. Moore, A. L. Moore, *Acc. Chem. Res.***1993**, *26*, 198.
[8] P. K. Dutta, M. Ledney, *Prog. Inorg. Chem.* **1997**, *44*, 209.
[9] D. W. Breck, *Zeolite Molecular Sieves: Structure, Chemistry and Use*, Wiley, New York, **1974**.
[10] *Zeolites and Related Materials: State of the Art* (Eds.: J. Weitkamp, H. G. Karge, H. Pfeifer, W. Holderich), Elsevier, **1994**.
[11] W. H. Quayle, J. H. Lunsford, *Inorg. Chem.* **1982**, *21*, 97.
[12] P. Laine, M. Lanz, G. Calziferri, *Inorg. Chem.* **1996**, *35*, 3514.
[13] K. Maruszewski, D. P. Strommen, K. Handrich, J. R. Kincaid, *Inorg. Chem.* **1991**, *30*, 4579.
[14] K. Maruszewski, D. P. Strommen, J. R. Kincaid, *J. Am. Chem. Soc.* **1993**, *115*, 8345.
[15] K. Maruszewski, J. R. Kincaid, *Inorg. Chem.* **1995**, *34*, 2002.
[16] W. Szulbinski, J. R. Kincaid, *Inorg. Chem.* **1998**, *37*, 859.
[17] A. Bhuiyan, J. R. Kincaid, *Inorg. Chem.* **1998**, *37*, 2525.
[18] A. Bhuiyan, J. R. Kincaid, *Inorg. Chem.* ***1999***, *38*, 4759.
[19] B. J. Coe, D. W. Thompson, C. D. Culbertson, J. R. Schoonover, T. J. Meyer, *Inorg. Chem.* **1995**, *34*, 3385.
[20] L. Persaud, A. J. Bard, A. Champion, M. A. Fox, T. E. Mallouk, S. E. Webber, J. M. White, *J. Am. Chem. Soc.* **1987**, *109*, 7309.
[21] P. K. Dutta, J. A. Incavo, *J. Phys. Chem.***1987**, *91*, 4443.
[22] P. K. Dutta, W. Turbeville, *J. Phys. Chem.* **1992**, *96*, 9410.
[23] Y. I. Kim, T. E. Mallouk, *J. Phys. Chem.* **1992**, *96*, 2879.
[24] E. H. Yamamoto, Y. I. Kim, R. H. Schmehl, J. O. Wallin, B. A. Shoulders, B. R. Richardson, J. F. Haw, T. E. Mallouk, *J. Am. Chem. Soc.* **1994**, *116*, 10557.
[25] P. K. Dutta, M. Borja, *Nature* **1993**, *362*, 43.
[26] M. Sykora, K. Maruszewski, S. M. Treffert-Ziemelis, J. R. Kincaid, *J. Am. Chem. Soc.***1998**, *120*, 3490.
[27] M. Sykora, J. R. Kincaid, *Nature* **1997**, *387*, 162.
[28] A. Bhuiyan, J. R. Kincaid, *Inorg. Chem.* submitted .
[29] D. Man′uel, W. Szulbinski, J. R. Kincaid, *J. Am. Chem. Soc.* submitted.
[30] R. J. Crutchley, A. B. P. Lever, *Inorg. Chem.***1982**, *21*, 2276.
[31] M. Sykora, J. R. Kincaid, P. K. Dutta, N. B. Castagnola, *J. Phys. Chem.***1999**, *103*, 309.

  0947-6539/00/0622-4061 $ 17.50+.50/0